

Supporting Information

Interaction of Mixed-Ligand Monolayer-Protected Au₁₄₄ Clusters with Biomimetic Membranes as a Function of the Transmembrane Potential

Lucia Becucci,[‡] Rolando Guidelli,[‡] Federico Polo,[§] and Flavio Maran[§]

[‡]Department of Chemistry, Florence University, 50019 Sesto Fiorentino (Firenze), Italy

[§]Department of Chemistry, University of Padova, 35131 Padova, Italy

Table of Contents:

1. Methods
2. Chemicals
3. Synthesis
4. Electrochemistry
5. Figures
6. References

1. Methods

Melting points were determined with a Leitz model Laborlux 12. Analytical thin-layer chromatography (TLC) was performed by using silica-gel 60 F₂₅₄ plates (Merck). The solid-state (KBr disk) IR absorption spectra were recorded with a Perkin-Elmer model 1720X FT-IR spectrophotometer, nitrogen-flushed, equipped with a sample-shuttle device, at 2 cm⁻¹ nominal resolution, averaging over 100 scans. UV-vis spectra were obtained with a Varian Cary 5 UV-vis spectrophotometer. Mass spectroscopy (electrospray ionization, ESI-MS) was performed by using a PerSeptive Biosystem

Mariner instrument. Thermogravimetric analysis (TGA) was carried out with a Hi-Res Modulated TGA 2950 Thermogravimetric Analyzer (TA Instruments) working in Hi-Res Ramp mode: ramp 1.5 – 50 °C/min (depending on the rate of mass loss with temperature), resolution 4. TGA curves were recorded under a working N₂ flux equal to 100 ml min⁻¹ in the range 25 to 600 °C. The measurements were carried out on carefully dried, accurately weighed 4-5 mg samples and in an open platinum pan. Transmission electron microscopy (TEM) phase contrast images were obtained with a JEOL JEM 2010 microscope operating at 200 keV. Droplets of the MPC solutions were drop cast on standard carbon-coated (20-30 nm) Formvar films on copper grids (400 mesh) and dried. Histograms of the core sizes and corresponding Gaussian fit to the data were obtained from digitized images. ¹H NMR spectra were obtained with a Bruker model AC 200 spectrometer, a Bruker model AM Avance 400 spectrometer, or a Bruker model Avance DRX-600 spectrometer. Deuteriochloroform (99.8%, *d*; Aldrich), deuterated methanol (99.8%, *d*₄; Aldrich), and deuterated dimethyl sulfoxide (99.9%, *d*₆; Aldrich) were used as the solvents. Chemical shifts (δ) are reported as part per million (ppm) downfield from tetramethylsilane.

2. Chemicals

The following reagents and solvents were commercially available and used as received. Trifluoroacetic acid 99%, triisopropylsilane 99%, (Acros Organics). 5-Bromovaleric acid 97%, tetra-*n*-octylammonium bromide 98%, sodium borohydride 99.9%, tetrachloroauric acid trihydrate (HAuCl₄·3H₂O) 99.9+%, triphenylmethanethiol 97%, 8-bromooctanoic acid 97%, potassium methoxide 95%, dimethylaminopyridine 99% (DMAP), phenylethanethiol 98%, sodium methoxide purum, dimethylsulfoxide (DMSO), cadmium sulfate (Sigma-Aldrich). 1-[3-(dimethylamino)-propyl]-3-ethylcarbo-diimide hydrochloride (EDC·HCl) (GL Biochem, Shanghai). Potassium bisulfate, sodium bicarbonate, sodium sulfate anhydrous, acetonitrile, diethyl ether, ethanol, ethyl acetate, methanol, methylene chloride, petroleum ether, toluene (Carlo Erba). Potassium dihydrogen phosphate and potassium hydrogen phosphate, suprapur[®] potassium chloride

(Merck, Darmstadt, Germany); the latter was baked at 500°C before use to remove any organic impurities. For the synthesis of gold nanoclusters, low-conductivity water was obtained using deionized water, which was further treated with the Milli-Q purification system. For electrochemical measurements, water was obtained by an inverted osmosis unit, distilled once and then redistilled from alkaline permanganate. Dioleoylphosphatidylcholine (DOPC) was purchased in chloroform solution from Avanti Polar Lipids (Birmingham, AL, U.S.A.). The 2,3-di-O-phytanyl-sn-glycerol-1-tetraethylene-glycol-D,L- α lipoic acid ester thiolipid (DPTL) was provided by Prof. Adrian Schwan (Department of Chemistry, University of Guelph, Canada). Solutions of 0.2 mg/ml DPTL in ethanol were prepared from a 2 mg/ml solution of DPTL in ethanol. Stock solutions of this thiolipid were stored at -18°C .

3. Synthesis

Au₁₄₄(SC₂H₄Ph)₆₀. The synthesis of Au₁₄₄(SCH₂CH₂Ph)₆₀ was carried out according to a literature method.^{S1} HAuCl₄•3H₂O (2 g, 5.05 mmol) was dissolved in 60 ml water. 145 ml toluene and 3.20 g (5.85 mmol) tetra-*n*-octylammonium bromide were then added. After 30 min stirring, the clear aqueous phase was removed and the dark-red toluene solution was cooled to 0 °C. Phenylethanethiol (3.62 ml, 27 mmol) was added to the toluene solution, under slow stirring. When the solution became opaque white, 2.4 g sodium borohydride (63.4 mmol), dissolved in 30 ml of ice-cold water, was added under vigorous stirring with immediate formation of a black color pointing to formation of AuNPs. The reaction mixture was let to warm up to room temperature and stirred for 1 day. The solution was washed with water (3 x 100 ml) in a separatory funnel and toluene was then evaporated to leave a black product. Excess thiol was removed by adding ethanol to the crude product, and the supernatant was then discarded. These ethanol steps were repeated thrice. The reaction also forms (*n*-Oct₄N⁺)[Au₂₅(SC₂H₄Ph)₁₈][−], which could be removed from the solid by washing with acetonitrile (10 x 10 ml). The final product, Au₁₄₄(SC₂H₄Ph)₆₀, was obtained as a black powder. Its purity was assessed by electrochemistry,^{S2} and UV-vis and ¹H NMR spectroscopies.^{S1}

Ph₃C-S-(CH₂)₇COOH (1). Acid **1** was prepared according to a literature procedure.^{S3} Sodium methoxide (3.5 M solution in methanol, 1.1 ml, 3.85 mmol) was slowly added to a solution of triphenylmethanethiol (0.513 g, 1.86 mmol) in toluene (1 ml). To this mixture, a solution of 8-bromooctanoic acid (0.401 g, 1.80 mmol) in methanol (1 ml) was slowly added at 5-10 °C. The mixture was allowed to warm to 50 °C and was then stirred for 2 h. During this time, the extent of reaction was checked by TLC and a second mixture of triphenylmethanethiol (0.238 mg, 0.86 mmol in 0.5 ml of toluene) and sodium methoxide (3.5 M solution in methanol, 0.5 ml, 1.92 mmol) were added to increase the reaction yield further. The solvent mixture was removed under reduced pressure, and the residue dissolved in 30 ml of water. The aqueous solution was acidified (pH ~ 5-6) with 0.1 M H₂SO₄ and extracted with ethyl acetate (3 x 10 ml). The combined extracts were dried over Na₂SO₄ and concentrated under reduced pressure. The crude material was purified by flash chromatography (methylene chloride) to afford 0.480 g of **1** as a yellow oil. Yield: 64%; ¹H NMR (CDCl₃) δ 1.10-1.68 (m, 10H, 5CH₂), 2.13 (t, 2H, S-CH₂), 2.31 (t, 2H, CH₂-CO), 7.20-7.44 (m, 15H, 3Ph).

HS-(CH₂)₇COOH (2). Compound **1** (0.078 g, 0.19 mmol) was dissolved in 4 ml of a 7:2:1 mixture of CH₂Cl₂/trifluoroacetic acid/triisopropylsilane. The solution was stirred for 2 h at room temperature and then the solvent was evaporated. The crude product was washed with diethyl ether to remove the excess of trifluoroacetic acid by evaporation. Then, after addition of 3 ml of 5% NaHCO₃, triphenylmethane was removed by extraction with ethyl acetate (3 x 1 ml). The aqueous phase was acidified with 10% KHSO₄ and extracted with ethyl acetate (3 x 1 ml). The combined extracts were dried over Na₂SO₄ and concentrated under reduced pressure to yield **2** as a yellow oil. Yield: 87%; ¹H NMR (CDCl₃) δ 1.10-1.68 (m, 10H, 5CH₂), 2.36 (t, 2H, CH₂-CO), 2.58 (m, 2H, S-CH₂), 2.67 (t, 1H, SH).

Ph₃C-S-(CH₂)₅COOH (3). Potassium methoxide (3.5 M solution in methanol, 3.4 ml, 11.9 mmol) was slowly added to a solution of triphenylmethanethiol (1.5 g, 5.43 mmol) in toluene (1 ml). To this mixture, a solution of bromovaleric acid (0.99 g, 5.48 mmol) in methanol (1 ml) was slowly added at 5-10 °C. The mixture was allowed to warm to 50 °C

and then stirred for 2 h. The solvent was removed under reduced pressure, and the residue was dissolved in 30 ml of water. The aqueous solution was acidified (pH ~ 5-6) with 0.1 M H₂SO₄ and extracted with ethyl acetate (3 x 10 ml). The combined extracts were dried over Na₂SO₄ and concentrated under reduced pressure. The product was purified by crystallization from ethyl acetate/petroleum ether. Yield: 55%; mp 127-128 °C; IR (KBr) ν_{\max} 3424, 3083, 3030, 1701, 1592 cm⁻¹; ¹H NMR (CDCl₃) δ 1.42 (m, 2H, CH₂), 1.58 (m, 2H, CH₂), 2.14-2.23 (m, 4H, α -CH₂ and β -CH₂), 7.19-7.29 (m, 10H, 2Ph), 7.41 (m, 5H, Ph).

***n*Oct-Aib-Gly-Leu-Aib-Gly-Gly-Leu-Aib-Gly-Ile-Lol-O-CO-(CH₂)₄-S-Trt (trichogin GA IV-STrt, 4).** Trichogin GA IV, *n*Oct-Aib-Gly-L-Leu-Aib-Gly-Gly-L-Leu-Aib-Gly-L-Ile-L-Lol,^{S4,S5} was available from a previous study.^{S6} **3** (0.09 g, 0.23 mmol) and DMAP (0.03 g, 0.23 mmol) were added to a cold solution (0 °C) of trichogin GA IV (0.27 g, 0.19 mmol) in anhydrous CH₂Cl₂. After 10 min, EDC·HCl (0.075 g, 0.34 mmol) was added to the solution, the pH was adjusted to 8 with DMAP, and the mixture was allowed to react under stirring at room temperature for 4 days. The solvent was removed under reduced pressure and the residue dissolved in ethyl acetate. The solution was washed with 10% KHSO₄, water, 5% NaHCO₃, and water, dried over Na₂SO₄ and evaporated to dryness. **4** was obtained in 83% yield; mp: 110-111 °C; [α]_D²⁰: -11.3° (c = 0.1, MeOH); IR (KBr) ν_{\max} 3335, 1660, 1652, 1537 cm⁻¹; ¹H NMR (600 MHz, DMSO-d₆) δ (the residues are numbered according to the trichogin sequence) 0.77-0.88 (m, 27H, 6 δ -CH₃, Leu_[3], γ -CH₃, Ile, δ -CH₃, Ile, ω -CH₃, *n*Oct), 1.07 (m, 1H, γ -CH₂, Ile), 1.24 (m, 10H, *n*Oct (CH₂)₅), 1.31-1.38 (m, 18H, 6 β -CH₃, Aib_[3]), 1.40-1.42 (m, 4H, β -CH₂, γ -CH₂), 1.60-1.62 (m, 10H, β -CH₂, Leu_[3], γ -CH, Leu_[3]; 1H γ -CH₂, Ile), 1.81 (m, 1H, β -CH, Ile), 2.07-2.14 (m, 4H, α -CH₂, δ -CH₂), 3.57 (s, 3H, OMe), 3.59-3.76 (m, 10H, α -CH₂, Gly_[4]; CH₂OH, Lol), 3.93 (m, 1H, α -CH), 4.07 (m, 2H, α -CH, Leu_[2]), 4.17 (m, 1H, α -CH), 4.21 (m, 1H, α -CH), 7.23-7.25 (m, 5H, Ph), 7.32-7.35 (m, 10H, 2Ph), 7.42 (d, 1H, NH), 7.62 (d, 1H, NH), 7.75-7.77 (m, 2H, 2 NH), 7.83-7.85 (m, 2H, 2NH), 7.88 (t, 1H, NH, Gly), 7.92 (t, 1H, NH, Gly), 8.00 (s, 1H, NH, Aib), 8.30 (t, 1H, NH, Gly), 8.43 (s,

1H, NH, Aib); MS (ESI-MS): $[M+H]^+_{\text{calc}} = 1423.87$; $[M+H]^+_{\text{exp}} = 1423.86$; $[(M-\text{Trt})+H]^+_{\text{exp}} = 1182.76$.

***n*Oct-Aib-Gly-Leu-Aib-Gly-Gly-Leu-Aib-Gly-Ile-Lol-O-CO-(CH₂)₄-S-H (trichogin GA IV-SH, **5**).** **4** was dissolved in 5 ml of a 7:2:1 mixture of CH₂Cl₂/trifluoroacetic acid/triisopropylsilane. The solution was stirred for 2 h at room temperature and then the solvent was evaporated. The product was washed with diethyl ether to remove the excess of trifluoroacetic acid by evaporation. The crude product was dried in vacuo for 12 h, over KOH pellets, and crystallized from diethyl ether to give **5** as a colorless solid (yield = 80%), which was immediately used as such for the preparation of functionalized MPCs.

Au₁₄₄OctA. Au₁₄₄(SC₂H₄Ph)₆₀ (0.094 g, 2.57×10^{-3} mmol) was dissolved in CH₂Cl₂ (10 ml) and HS-OctA (0.026 g, 0.15 mmol) was added under vigorous stirring. The dark brown solution was allowed to react for 24 h. CH₂Cl₂ was rotary evaporated and the resulting black solid was washed several times with acetonitrile and dried. The solid was then washed several times with petroleum ether and then dried to yield the modified MPC. The exchanged MPC shows good solubility in polar solvent such as ethanol, methanol, dimethyl sulfoxide (DMSO), DMF, whereas the native cluster does not.

Au₁₄₄TCG. Au₁₄₄(SC₂H₄Ph)₆₀ (0.108 g, 2.95×10^{-3} mmol) was dissolved in CH₂Cl₂ (10 ml) and the thiolated trichogin (0.162 g, 0.15 mmol) was added under vigorously stirring. The dark brown solution was allowed to react for 24 h. The solvent was evaporated and the dark brown solid was washed several times with acetonitrile, and then dried carefully to yield the desired product. The exchanged MPC is soluble in the same polar solvents as the previous octanoic-acid modified cluster.

4. Electrochemistry

For the electrochemical characterization of the modified clusters, the working electrode was a 0.55 mm radius glassy carbon (GC) disk prepared as already described.^{S7} Before use, the electrode was polished with 0.25 μm diamond paste (Struers), ultrasonically rinsed with ethanol for 5 min, washed with acetone, and carefully dried with a cold air stream. The GC electrode was activated in the background solution, DMF containing 0.1

M tetra-*n*-butylammonium hexafluorophosphate (TBAH), by means of several voltammetric cycles at a scan rate of 0.5 V s^{-1} between the positive and the negative potential limits of concern. The electrochemical area, $9.64 \times 10^{-3} \text{ cm}^2$, was determined with reference to low scan rate voltammetric oxidation of ferrocene in DMF/0.1 M tetra-*n*-butylammonium perchlorate, in which ferrocene has a diffusion coefficient of $1.13 \times 10^{-5} \text{ cm}^2 \text{ s}^{-1}$. A Pt wire was the counter electrode and an Ag wire served as a quasi-reference electrode. At the end of the experiments, the potential of the Ag quasi-reference electrode was calibrated against the ferricenium/ferrocene (Fc^+/Fc) redox couple (in the same solvent/electrolyte system, $E^\circ_{\text{Fc}/\text{Fc}^+} = 0.464 \text{ V}$ against the KCl saturated calomel electrode, SCE);^{S7} potential values are reported against SCE. The differential pulse voltammetry (DPV) experiments were carried out with a CHI 760d electrochemical workstation. We used peak amplitude of 50 mV, pulse width of 0.05 s, 2 mV increment per cycle, and pulse period of 0.1 s.

The experiments with supported monolayers and bilayers were carried out on the native $\text{Au}_{144}(\text{SC}_2\text{H}_4\text{Ph})_{60}$ cluster and the two exchanged clusters, $\text{Au}_{144}\text{OctA}$ and $\text{Au}_{144}\text{TCG}$. Stock solutions (1 mg ml^{-1}) of these MPCs were prepared by dissolving $\text{Au}_{144}\text{OctA}$ and $\text{Au}_{144}\text{TCG}$ in DMSO, and dispersing $\text{Au}_{144}(\text{SC}_2\text{H}_2\text{Ph})_{60}$ in ethanol. Measurements were carried out with a homemade HMDE, described elsewhere.^{S8} A homemade glass capillary with a finely tapered tip, about 1 mm in outer diameter, was employed. To avoid any changes in drop area due to a change in temperature, capillary and mercury reservoir were thermostatted at $25 \pm 0.1 \text{ }^\circ\text{C}$ in a water-jacketed box. The HMDE was the working electrode in a three-electrode system, with an Ag/AgCl (0.1 M KCl) reference electrode and a platinum-coil counter electrode. Mercury-supported lipid SAMs were obtained by spreading a DOPC solution in pentane on the surface of a 0.1 M KCl aqueous solution, in an amount corresponding to about five phospholipid monolayers. After allowing the pentane to evaporate, the HMDE was immersed into the aqueous solution across the lipid film. This procedure gives rise to a lipid monolayer with the hydrocarbon tails directed toward the mercury surface and the polar heads directed toward the aqueous solution, thanks to the hydrophobic nature of mercury. The lipid monolayer is at its equilibrium

spreading pressure.^{S9} Mercury-supported tBLMs were obtained by tethering a DPTL monolayer to the HMDE upon keeping the mercury drop immersed in a 0.2 mg ml⁻¹ DPTL solution in ethanol for about 20 min. A DOPC monolayer was then formed on top of the DPTL monolayer by a procedure analogous to that employed for the preparation of the previous Hg-supported monolayer, and consisted in spreading a DOPC solution in pentane on the surface of a 0.1 M KCl aqueous solution. Immersion of the DPTL-coated mercury into the aqueous solution across the DOPC film causes a lipid monolayer to self-assemble on top of the DPTL monolayer, thanks to the hydrophobic interactions between the alkyl chains of the phospholipid and those of the thiolipid. The tBLM was then subjected to repeated potential scans over a potential range from -0.2 to -1.2 V, while continuously monitoring the curve of the quadrature component of the current at 75 Hz against the applied potential, E , using AC voltammetry, until a stable curve was attained. The MPCs were then injected into the working electrolysis cell from their solutions in DMSO or ethanol in an amount of 2 or 4 $\mu\text{g ml}^{-1}$; the resulting MPC solutions were initially clear, but they started sedimenting after several hours. The very small amount of organic solvent involved in these additions was found to have no detectable effect on the electrochemical response. No attempt was made to evaluate the influence of the MPC concentration in the DOPC SAM, due to the difficulty of estimating it with acceptable accuracy. Spreading a mixture of MPCs and DOPC of known composition on the surface of the working aqueous solution is complicated by the very low solubility of the MPCs in the liquid alkane used for spreading. Moreover, the solubility of Au₁₄₄OctA and Au₁₄₄TCG in aqueous solution is not entirely negligible, causing the mole fraction of these MPCs in the alkane after attainment of equilibrium conditions to be different from its pristine value. In addition, the above co-spreading procedure would prevent the good quality of the sole DOPC SAM to be checked by AC voltammetry before adding the MPCs to the aqueous solution.

Impedance spectroscopy and cyclic voltammetric measurements were carried out with an Autolab instrument PGSTAT12 (Echo Chemie) supplied with FRA2 module for impedance measurements, SCAN-GEN scan generator and GPES 4.9007 software.

Potentials were measured *vs.* a Ag|AgCl electrode immersed in the 0.1 M KCl working solution, which was buffered at pH 7 with a 10^{-3} M phosphate buffer, unless otherwise stated.

5. Figures

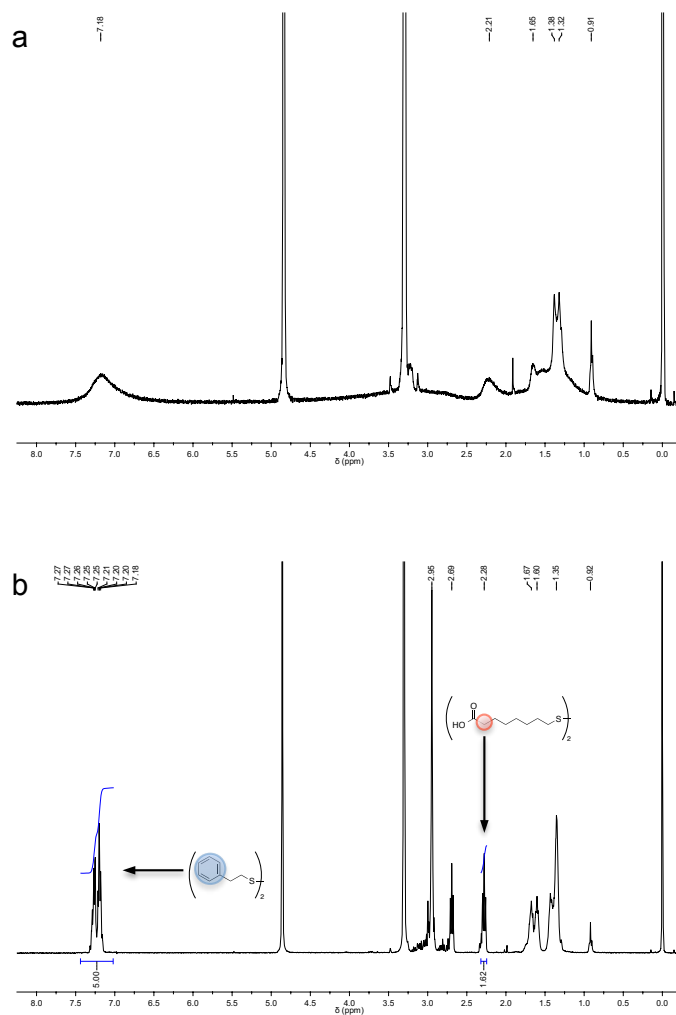


Figure S1. ^1H NMR of $\text{Au}_{144}\text{OctA}$ before (a) and after oxidative decomposition with an excess of iodine (b), in deuterated methanol. The molar ratio between the liberated ligands was obtained by comparing the integrals of the resonances of the phenyl signals (for $\text{SC}_2\text{H}_4\text{Ph}$; 5 H) and the resonance of the methylene adjacent to the carbonyl group (for S-OctA; 2 H), as indicated in the figure. According to this analysis, the extent of exchange is 52%.

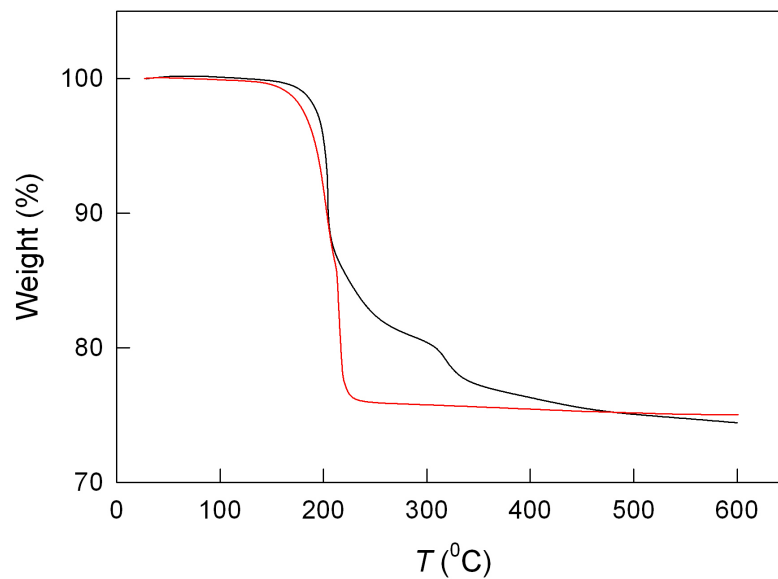


Figure S2. Hi-resolution TGA of Au₁₄₄OctA (black curve) compared to that of Au₁₄₄(SC₂H₄Ph)₆₀ (red curve). The phenylethanthiolate ligands undergo a desorption centered at ca. 205 °C, while the S-OctA ligands undergo a complex decomposition pattern starting from ca. 220 °C. The analysis indicated that the extent of exchange is 51%.

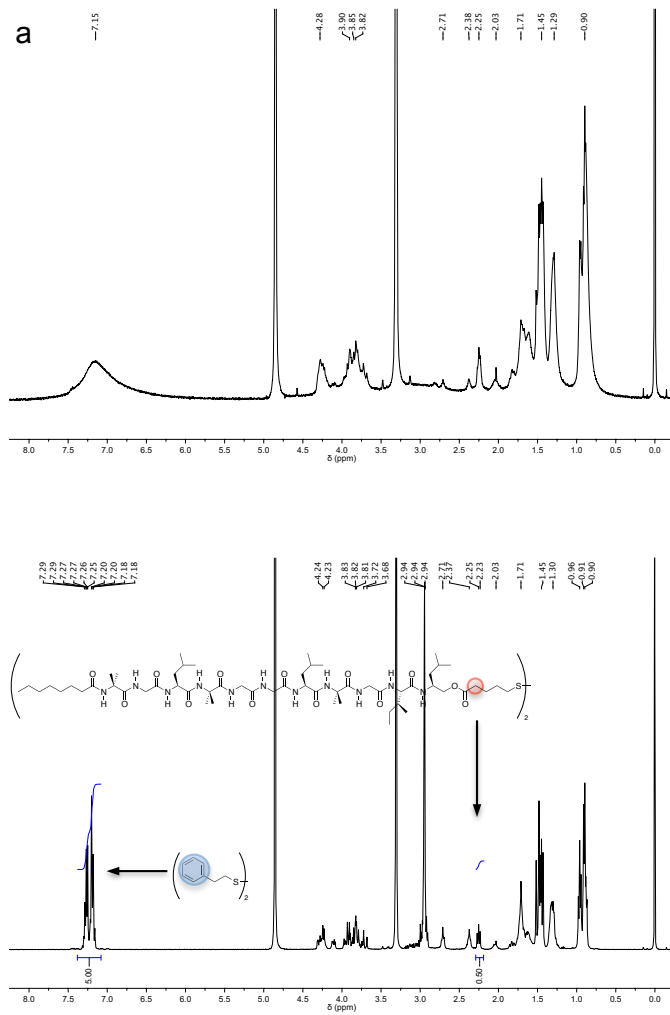


Figure S3. ¹H NMR of Au₁₄₄TCG before (a) and after oxidative decomposition with an excess of iodine (b), in deuterated methanol. The molar ratio between the liberated ligands was obtained by comparing the integrals of the resonances of the phenyl signals (for SC₂H₄Ph; 5 H) and the resonance of the methylene adjacent to the tether's carbonyl group (for thiolated trichogin GA IV; 2 H), as indicated in the figure. According to this analysis, the extent of exchange is 20%.

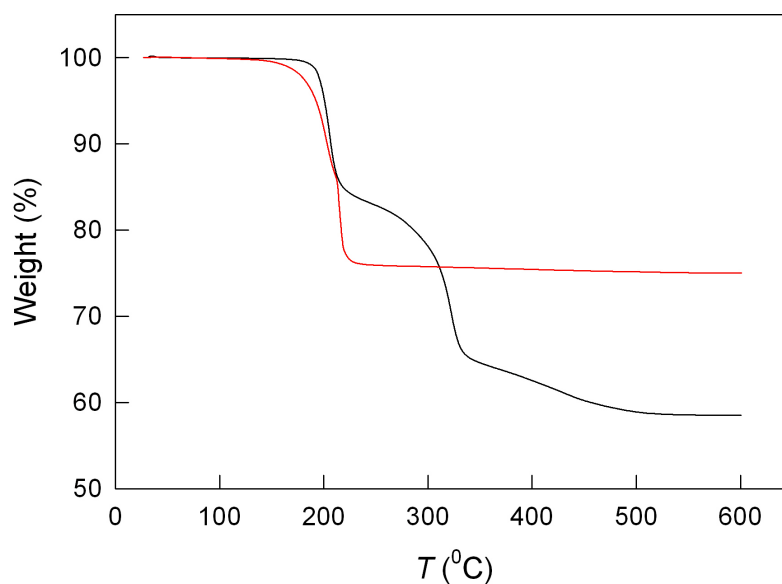


Figure S4. Hi-resolution TGA of $\text{Au}_{144}\text{TCG}$ (black curve) compared to that of $\text{Au}_{144}(\text{SC}_2\text{H}_4\text{Ph})_{60}$ (red curve). The phenylethanthiolate ligands undergo a sharp desorption centered at ca. 205 °C, while the thiolated trichogin ligands undergo a complex decomposition pattern starting from ca. 240 °C. The analysis indicated that the extent of exchange is 19%.

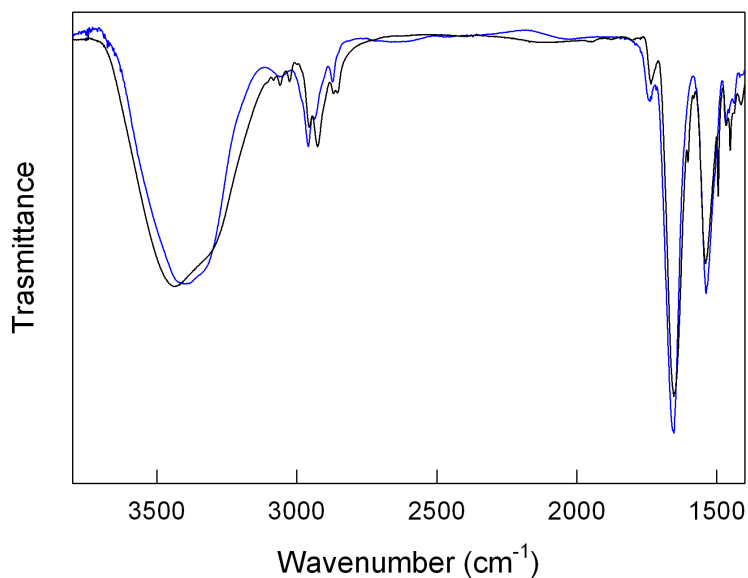


Figure S5. FT-IR in KBR of $\text{Au}_{144}\text{TCG}$ (black curve) and trityl-protected S-TCG (blue curve). The absorbance pattern of $\text{Au}_{144}\text{TCG}$ is similar to that of the thiolated TCG.

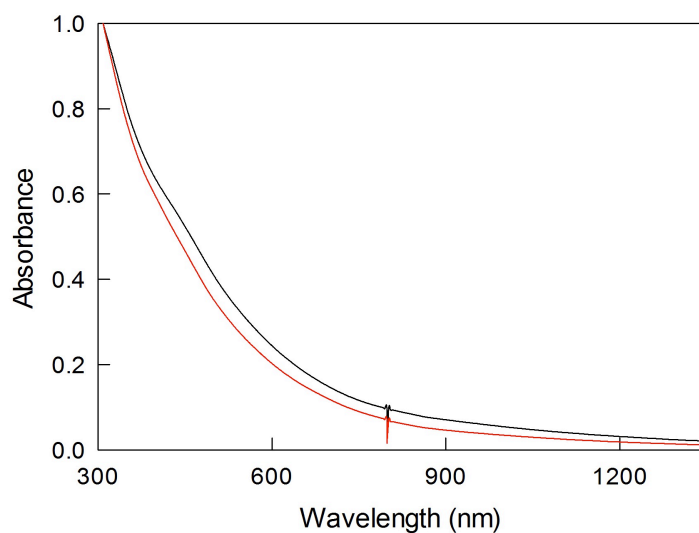


Figure S6. UV-vis absorption spectra of $\text{Au}_{144}\text{OctA}$ (black curve) and $\text{Au}_{144}(\text{SC}_2\text{H}_4\text{Ph})_{60}$ (red curve) in methanol and methylene chloride, respectively. The spectrum of $\text{Au}_{144}\text{OctA}$ maintains the same features as that of native $\text{Au}_{144}(\text{SC}_2\text{H}_4\text{Ph})_{60}$, which indicates that no size modification of the core occurred during the exchange reaction.

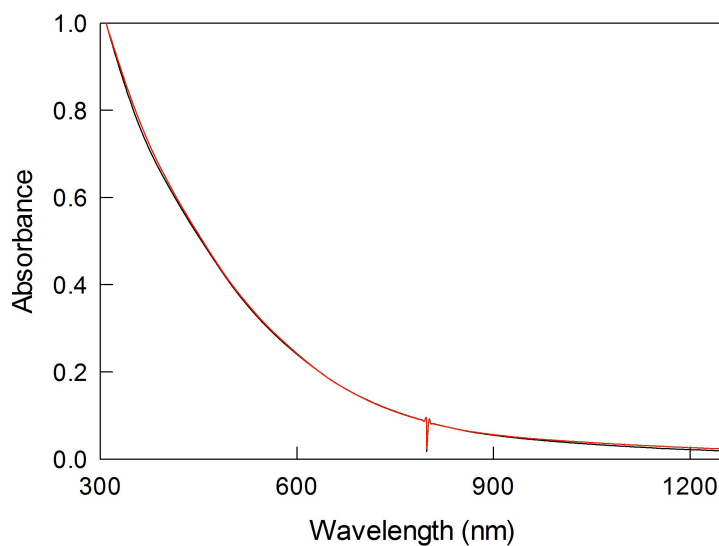


Figure S7. UV-vis absorption spectra of $\text{Au}_{144}\text{TCG}$ (black curve) and $\text{Au}_{144}(\text{SC}_2\text{H}_4\text{Ph})_{60}$ (red curve) in methanol and methylene chloride, respectively. The spectrum of $\text{Au}_{144}\text{TCG}$ maintains the same features as that of native $\text{Au}_{144}(\text{SC}_2\text{H}_4\text{Ph})_{60}$, which indicates that no size modification of the core occurred during the exchange reaction.

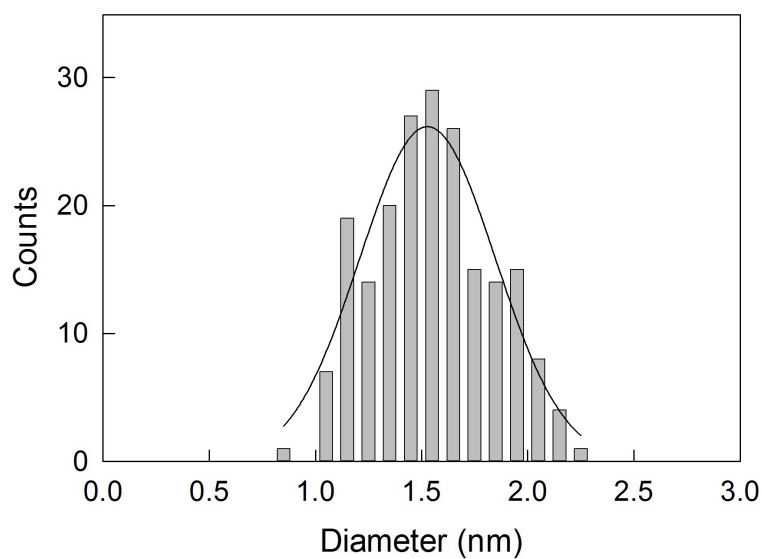


Figure S8. TEM analysis of Au₁₄₄OctA. Gaussian fit to the histogram (corresponding to images of 200 nanoclusters) yields an average core size of 1.60 nm, a standard deviation of 0.28 nm, and an average deviation of 0.23 nm.

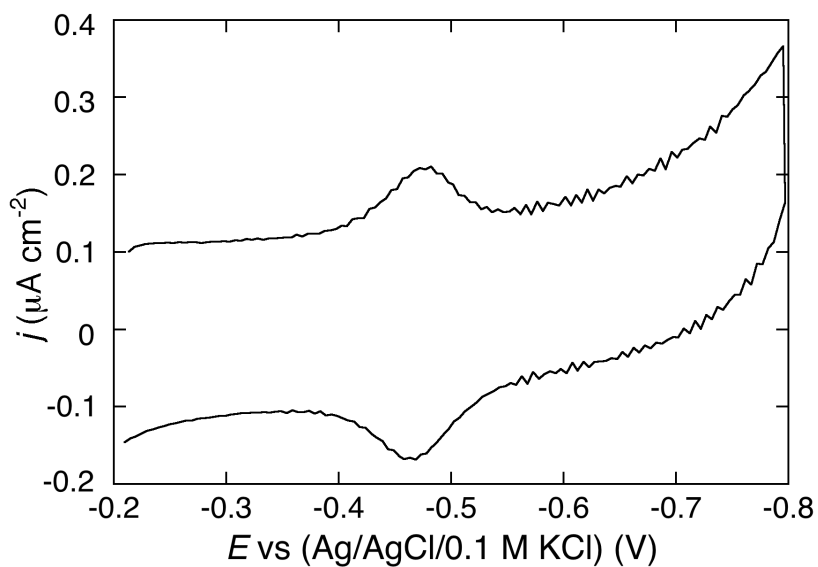


Figure S9. Cyclic voltammogram at a mercury-supported DOPC monolayer in a pH 7 buffer solution of 0.1 M KCl and 2 $\mu\text{g ml}^{-1}$ Au₁₄₄TCG. Scan rate = 50 mV s⁻¹.

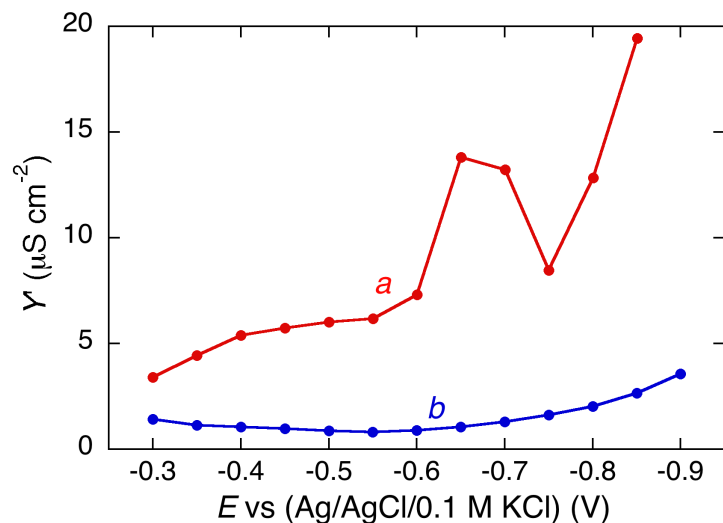


Figure S10. Curves of the in-phase component Y' of the admittance against E at 10 Hz on a mercury-supported DPTL/DOPC tBLM in a pH 7 buffer solution of 0.1 M KCl in the presence of 6 mg ml^{-1} of $\text{Au}_{144}(\text{SC}_2\text{H}_4\text{Ph})_{60}$ (a) and in its absence (b).

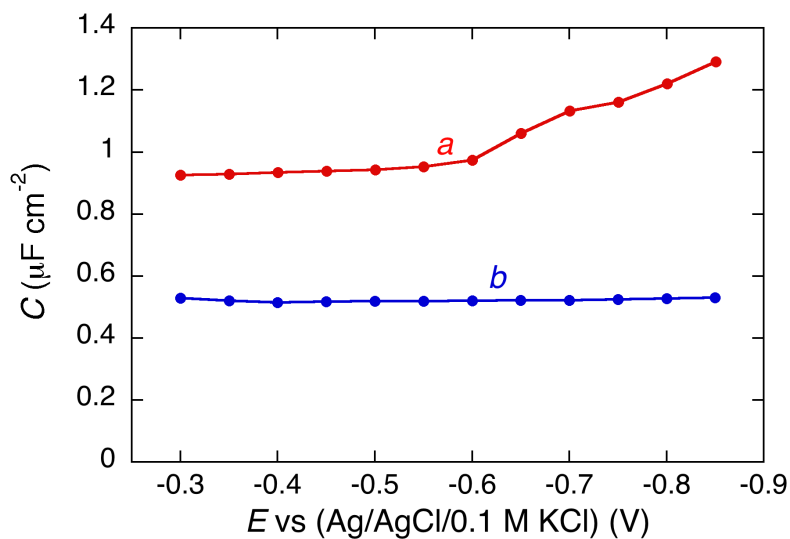


Figure S11. Curves of the differential capacitance C against E at 10 Hz on a mercury-supported DPTL/DOPC tBLM in a pH 7 buffer solution of 0.1 M KCl in the presence of 6 mg ml^{-1} of $\text{Au}_{144}(\text{SC}_2\text{H}_4\text{Ph})_{60}$ (a) and in its absence (b).

6. References

- S1. Donkers, R. L.; Lee, D.; Murray, R. W. Synthesis and Isolation of the Molecule-like Cluster $\text{Au}_{38}(\text{PhCH}_2\text{CH}_2\text{S})_{24}$. *Langmuir* **2004**, 20, 1945-1952.
- S2. Holm, A. H.; Ceccato, M.; Donkers, R. L.; Fabris, L.; Pace, G.; Maran, F. Effect of Peptide Ligand Dipole Moments on the Redox Potentials of Au_{38} and Au_{140} Nanoparticles. *Langmuir* **2006**, 22, 10584-10589.
- S3. Majer, P.; Jackson, P. F.; Delahanty, G.; Grella, B. S.; Ko, Y.-S.; Le, W.; Liu, Q.; Maclin, K. M.; Poláková, J.; Shaffer, K. A.; Stoermer, D.; Vitharana, D.; Wang, E. Y.; Zarkzeski, A.; Rojas, C.; Slusher, B. S.; Wozniak, K. M.; Burak, E.; Limsakun, T.; Tsukamoto, T. Synthesis and Biological Evaluation of Thiol-Based Inhibitors of Glutamate Carboxypeptidase II: Discovery of an Orally Active GCP II Inhibitor. *J. Med. Chem.* **2003**, 46, 1989-1996.
- S4. Toniolo, C.; Crisma, M.; Formaggio, F.; Peggion, C.; Monaco, V.; Goulard, C.; Rebuffat, S; Bodo, B. Effect of N^α-Acyl Chain Length on the Membrane-Modifying Properties of Synthetic Analogs of the Lipopeptaibol Trichogin GA IV. *J. Am. Chem. Soc.* **1996**, 118, 4952-4958.
- S5. Formaggio, F.; Peggion, C.; Crisma, M.; Toniolo, C. Short-chain Analogues of the Lipopeptaibol Antibiotic Trichogin GA IV: Conformational Analysis and Membrane Modifying Properties. *J. Chem. Soc., Perkin Trans. 2* **2001**, 1372-1377.
- S6. Becucci, L.; Maran, F.; Guidelli, R. Probing Membrane Permeabilization by the Antibiotic Lipopeptaibol Trichogin GA IV in a Tethered Bilayer Lipid Membrane. *Biochim. Biophys. Acta* **2012**, 1818, 1656-1662.
- S7. Antonello, S.; Musumeci, M.; Wayner, D. D. M.; Maran, F. Electroreduction of Dialkyl Peroxides. Activation–Driving Force Relationships and Bond Dissociation Free Energies. *J. Am. Chem. Soc.* **1997**, 119, 9541-9549.

S8. Moncelli, M. R.; Becucci, L. A Novel Model of the Hanging Mercury Drop Electrode. *J. Electroanal. Chem.* **1997**, *433*, 91-96.

S9. Bizzotto, D.; Nelson, A. Continuing Electrochemical Studies of Phospholipid Monolayers of Dioleoyl Phosphatidylcholine at the Mercury-electrolyte Interface. *Langmuir* **1998**, *14*, 6269-6273.